UNIVERSITÀ DEGLI STUDI DI MILANO
FACOLTÀ DI SCIENZE E TECNOLOGIE
CORSO DI LAUREA TRIENNALE IN FISICA
ANNO ACCADEMICO 2019/2020

Measurement of the inclusive isolated-photon yields in pp collisions at $\sqrt{s}$ =13 TeV with the ATLAS detector

Candidate: Davide Picchieri

Supervisors: Prof. Leonardo Carminati
Dott.ssa Silvia Resconi
Dott.ssa Federica Piazza

LHC and ATLAS Physics

- The Large Hadron Collider
  - The largest particle accelerator in the world
  - Centre-of-mass energy of 13 TeV
  - Instantaneous luminosity of $10^{34} cm^{-2} s^{-1}$
  - Objectives: test the Standard Model and look for new physics
- The Standard Model
  - A theory describing three of the four fundamental forces and the interactions among fermions shown in the table

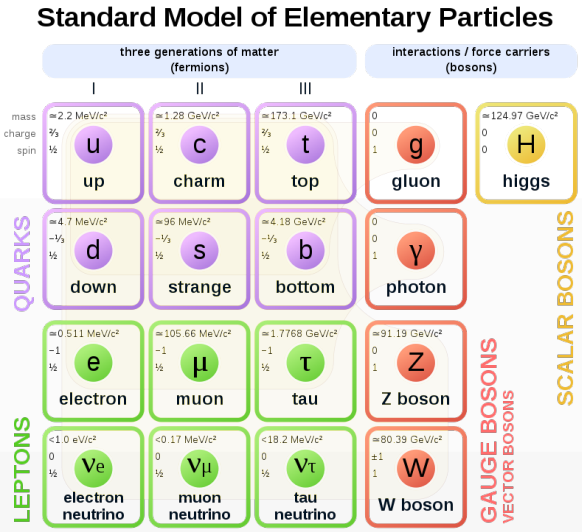

- Prompt Photon Production
  - Direct Photon: comes directly from hard interactions
  - Fragmentation Photon: it is the product of collinear fragmentation of a final state parton
- Aim of the Thesis
  - To measure the prompt photon yield
  - Subtract the background noise, usually final state jets mistaken as photons

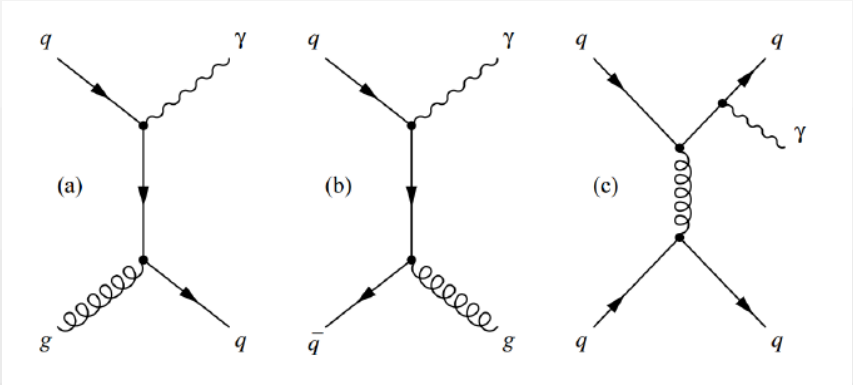

The ATLAS Detector

- The ATLAS Experiment
  - Located at one of the collision points between the beams of protons.
  - It is a general-purpose detector composed by three main systems
- The Inner Detector
  - Reconstructs the tracks of charged particle thanks to the Central Solenoidal Magnet (CSM)
- The Calorimeters
  - Located after the CSM and measure the energy lost by electrons, photons and hadrons as they pass through the detector.
  - Composed by an Electromagnetic Calorimeter and an Hadronic Calorimeter
- The Muon Spectrometer
  - Measures the muons thanks to some Toroidal Magnets dedicated to it
- The Trigger System
  - Level-1 Trigger is hardware based and selects up to 100'000 events per second
  - The High Level Trigger further selects the events to get to ~1000 events per second
- ATLAS coordinate system

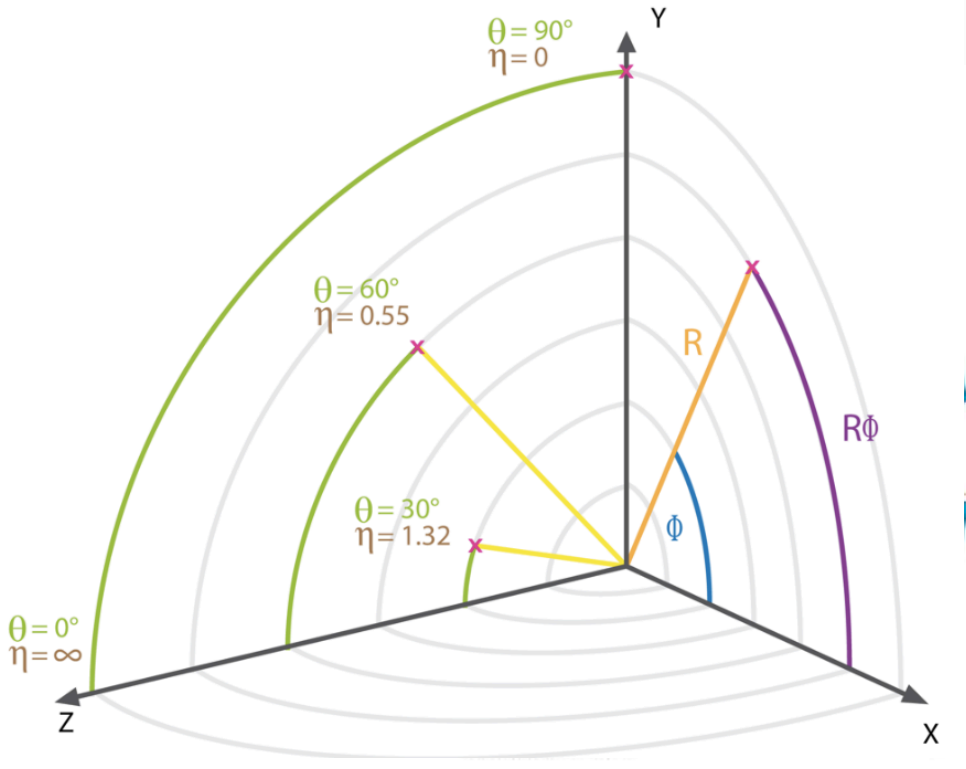

Photon Recontruction

- Reconstrucion starts from three separate steps:
  - Track reconstruction happens in the Inner Detector
  - Cluster Reconstruction happens in the EM Calorimeter via the Topo-Cluster Algorithm
  - Conversion Vertex Reconstruction happens in the Inner Detector

- A cluster is then matched with a track or a conversion vertex if possible
  - If it matches with a track it's reconstructed as an electron
  - If it matches to a conversion vertex as a converted photon
  - If it doesn't match with either as an unconverted photon

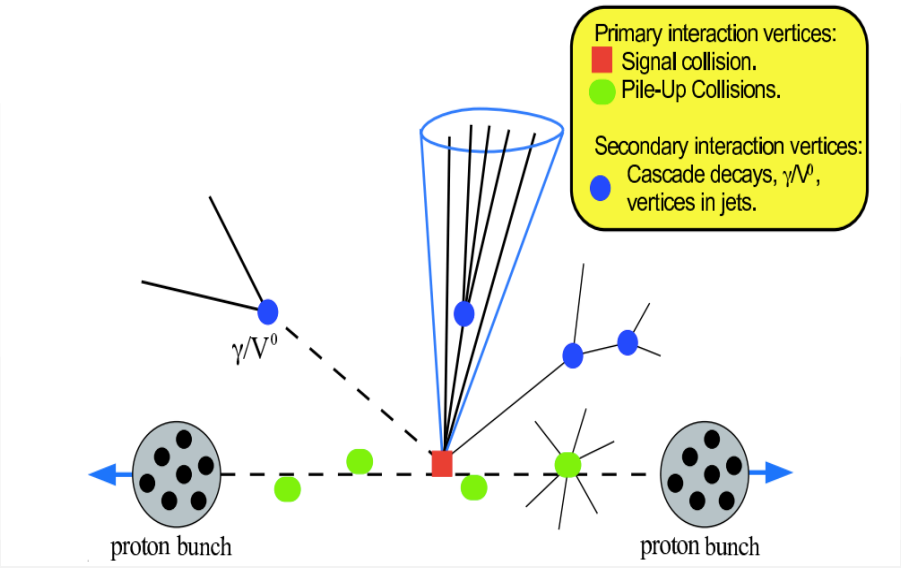

Photon Identification

- Identification of photon candidates
  - Relies on selections using calorimetric variables.
  - The loose selection is based on shower shapes in the second layer of the electromagnetic calorimeter and on the energy deposited in the hadronic calorimeter.
  - The tight selections, 9 in total, add information from the finely segmented strip layer of the calorimeter and are separately optimized for converted and unconverted photons

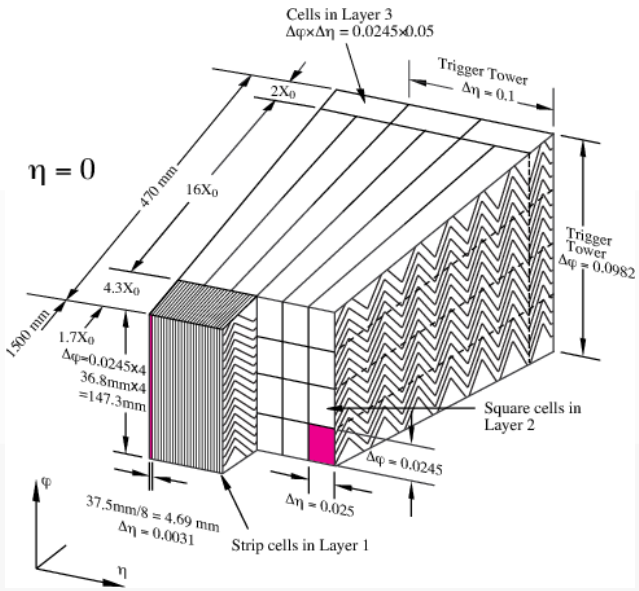

- Isolation of the photon candidate
  - Required to further reject background photons
  - Defined as the sum of transverse energy in topoclusters in the cone of radius $\Delta R = \sqrt{((\Delta\eta)^2+(\Delta\phi)^2)} < 0{,}4$
  - If it's smaller than $0.022p_T + 2.45$ GeV the photon fulfills the requirement

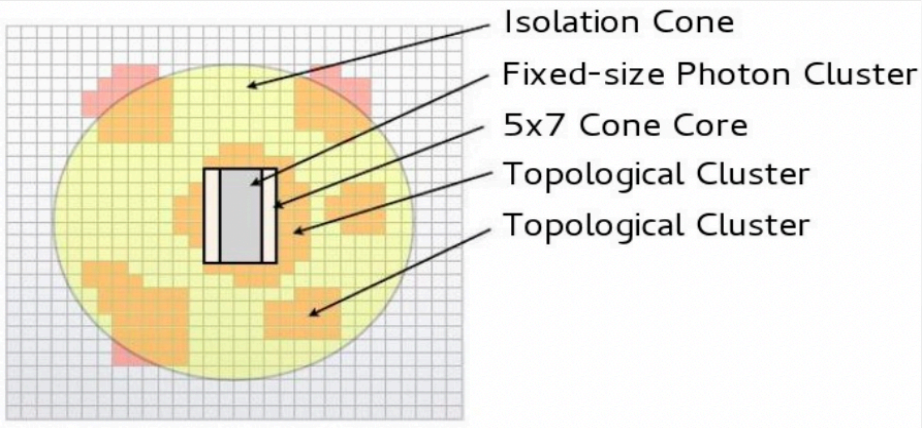

2-Dimensional Sideband Method

- Purity of the Signal
  - Fraction of true photons to the total number of photons in the signal region

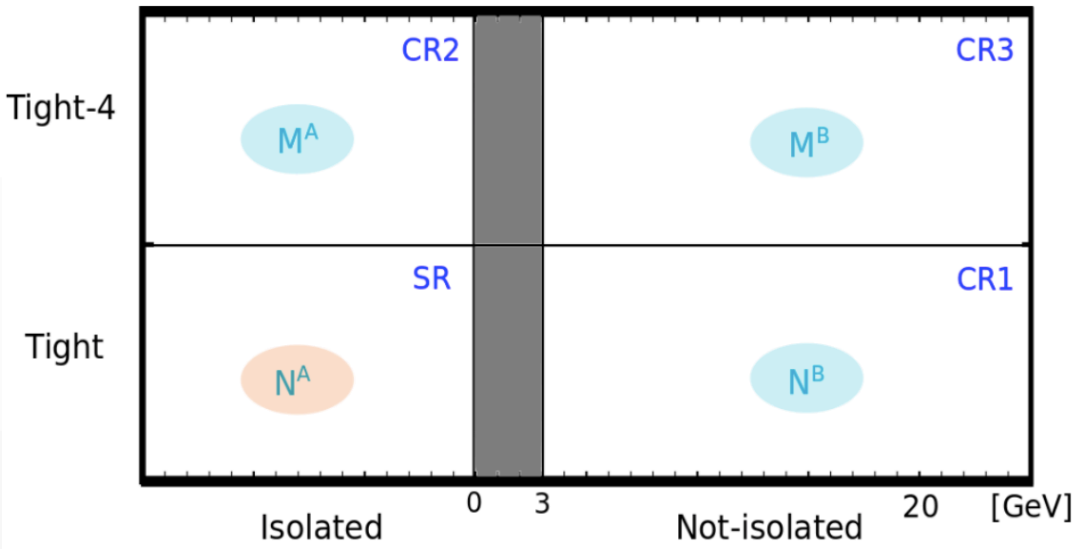

- Two starting hypotheses:
  - The correlation between the tightness and isolation is negligible: $N^A_{bkg} / N^B_{bgk} = M^A_{bkg} / M^B_{bkg}$
  - The number of true photons in the Control Regions is negligible in comparison to the number of fake photons: $N^B_{bkg} \gg N^B_{sig}$
  - The purity is then N^A_{sig}/N^A=1-$N^A M^B / N^B M^A$

2-Dimensional Sideband Method

- First MC input
  - Signal Leakage coefficients, account for the second hypothesis not being true
  - The assumption is taken that the ratios N^B_{sig}/N^A_{sig} M^A_{sig}/N^A_{sig} M^B_{sig}/N^A_{sig} are the same for the data and the MC simulation
  - These ratio are defined as c_i, SL coefficient from SR to CR1-3

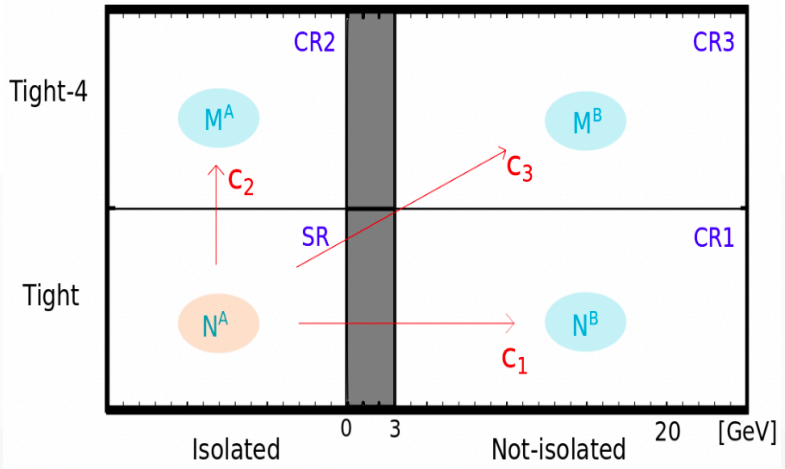

- Second MC input
  - Accounts for background correlation
  - Rewriting the background in the Signal Region as a function of the background in the other three regions and then uses the values found in the simulations
  - R_{MC} is $N^A_{bkg}M^B_{bkg}/N^B_{bkg}M^A_{bkg}$, and the signal is

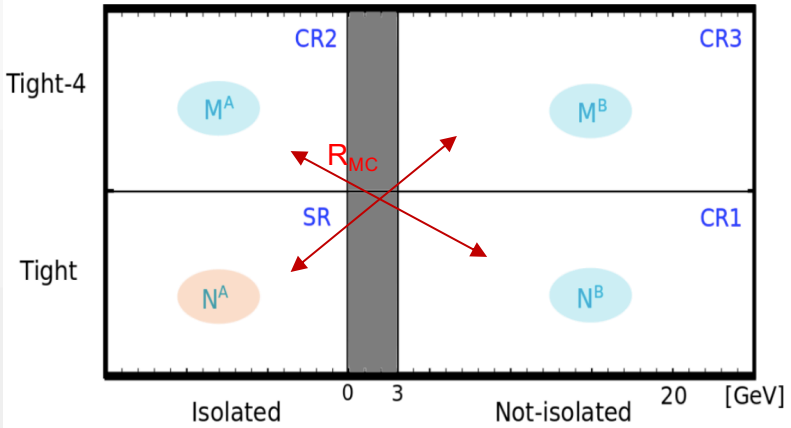

$$N^A_{sig} = \frac{(M^B + N^A c_3 - N^B c_2 R_{MC} - M^A c_1 R_{MC})(-1 + \sqrt{1 + \frac{4(c_1 c_2 R_{MC} - c_3)(N^A M^B - N^B M^A R_{MC})}{(M^B + N^A c_3 - N^B c_2 R_{MC} - M^A c_1 R_{MC})^2}}}{2(c_1 c_2 R_{MC} - c_3)}$$

Data processing

- For this study analysis software was configured in order to process the ATLAS data format in a more compact format (ROOT files)

- The production was run in batch mode on the Milano Tier3 computing facility via HTCondor to handle the high amount of data

- The total CPU time used for processing the 2015-2016 data with an integrated luminosity of 36 fb^{-1} is ~1500 h, for a total of ~$4x10^7$ events

- The total CPU time used for processing the data from PYTHIA and SHERPA event generator simulations is ~ 600 h each, for a total of ~10^7 Events each

Signal Leakage coefficients

- The trend of the Signal Leakage coefficients is shown in the following two tables, one for Barrel and one for End-Cap

Signal Leakage coefficients in Barrel

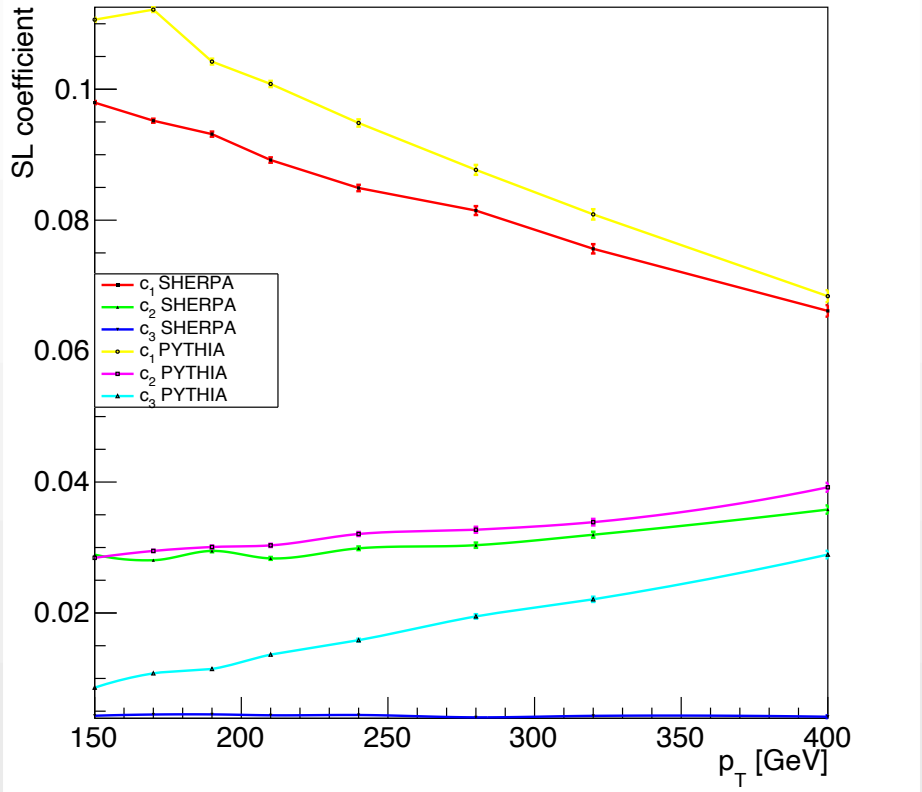

Signal Leakage coefficients in Endcap

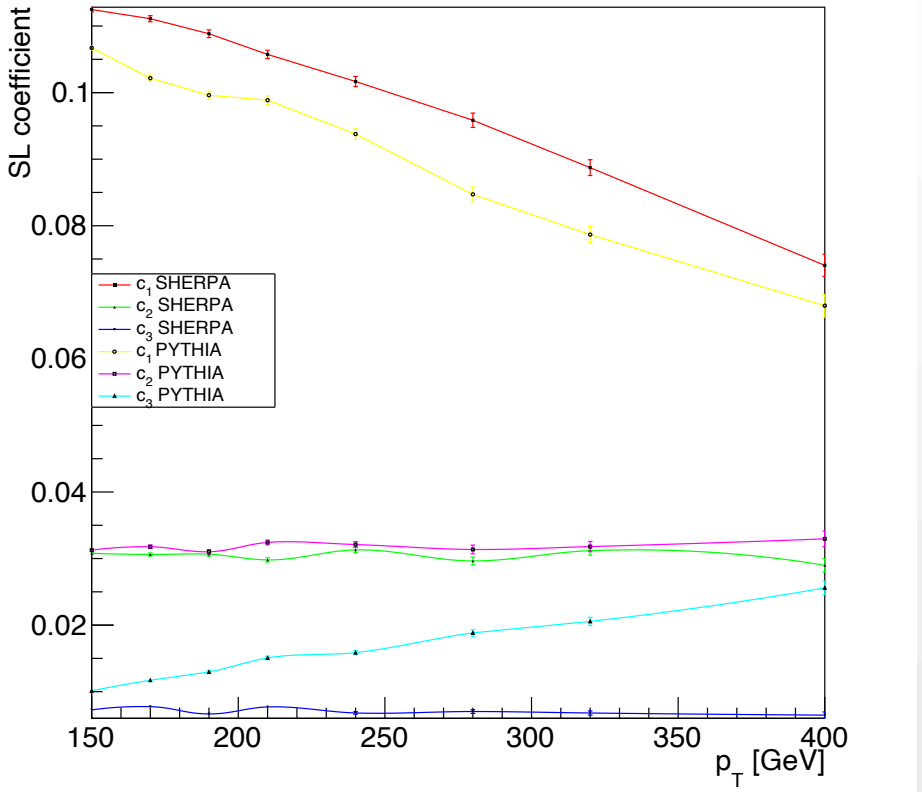

Correlation Factor for PYTHIA

- Since the R coefficients shows fluctuasions in the different regions of the $\eta - p_T$ space due to the limited number of events in each region, it seemed more reasonable to use the value calculated over the whole data set

Detector	p_T^γ [GeV]	R_{MC}	$\sigma\ R_{MC}$	R_{MC}^{BARREL}	$\sigma\ R_{MC}^{BARREL}$	R_{MC}^{pT}	$\sigma\ R_{MC}^{pT}$	R_{MC}^{SB}	$\sigma\ R_{MC}^{SB}$	Events
Barrel	150 - 170	1.6934	0.053	1.797	0.065	1.98	0.26	2.00	0.32	1004.88
	170 - 190					1.59	0.22	2.39	0.38	1101.58
	190 - 210					1.37	0.19	1.76	0.29	928.494
	210 - 240					1.66	0.25	1.52	0.26	1091.63
	240 - 280					1.73	0.25	1.61	0.27	1138.72
	280 - 320					1.36	0.22	1.13	0.21	867.477
	320 - 400					2.50	0.41	3.19	0.59	929.398
	400 - 900					1.31	0.23	1.46	0.28	941.057
Detector	p_T^γ [GeV]	R_{MC}	$\sigma\ R_{MC}$	R_{MC}^{ENDCAP}	$\sigma\ R_{MC}^{ENDCAP}$	R_{MC}^{pT}	$\sigma\ R_{MC}^{pT}$	R_{MC}^{SB}	$\sigma\ R_{MC}^{SB}$	**Events**
End-Cap	150 - 170	1.694	0.053	1.409	0.089	1.984	0.262	1.67	0.40	358.521
	170 - 190					1.59	0.22	0.42	0.13	338.838
	190 - 210					1.37	0.19	0.74	0.19	357.465
	210 - 240					1.66	0.25	2.21	0.65	347.606
	240 - 280					1.73	0.25	2.15	0.62	342.481
	280 - 320					1.36	0.22	2.52	0.86	233.061
	320 - 400					2.51	0.41	0.73	0.33	246.089
	400 - 900					1.32	0.23	0.79	0.36	180.53

Selection Process

- The events must satisfy beam, detector and data-quality criteria:
  - Triggering requirement on the loose photon candidate transverse energy (E_T^γ>140 GeV)
  - Loose identification requirements
  - Needs to satisfy $|\eta| < 1.37$ or $1.52 < |\eta| < 1.37$ to avoid the crack region and $p_T > 150$ GeV
  - Tight selections as described before
  - Isolation requirement by imposing Isolation < $0{,}022 p_T + 2.45$ GeV

	Loose selection	Cinematic selection	Tight selection	Isolation selection
Data	4.36×10^7	4.34×10^7	1.16×10^7	7.06×10^6
PYTHIA	9.39×10^6	9.38×10^6	8.44×10^6	7.47×10^6
SHERPA	1.10×10^7	1.10×10^7	1.03×10^7	9.26×10^6
PYTHIA weighted	7.82×10^6	7.82×10^6	7.14×10^6	6.08×10^6
SHERPA weighted	9.18×10^6	9.17×10^6	8.70×10^6	7.62×10^6

Purity and Systematic Errors

PYTHIA 1.186

p_T^γ [GeV]	Purity	Stat Error	Syst Error					Total Syst Error	Total Error
			c_1	c_2	c_3	Isolation	Tightness		
150 - 170	0.86	0.00051	0.0062	0.00088	0.00099	0.0028	0.069	0.069	0.069
170 - 190	0.87	0.00068	0.0072	0.0012	0.0012	0.0027	0.066	0.066	0.066
190 - 210	0.88	0.00089	0.0046	0.00028	0.0011	0.0027	0.065	0.065	0.065
210 - 240	0.89	0.00097	0.0041	0.0018	0.0014	0.0025	0.066	0.066	0.066
240 - 280	0.90	0.0012	0.0030	0.0012	0.0015	0.0023	0.070	0.070	0.070
280 - 320	0.90	0.0018	0.0035	0.0014	0.0018	0.0025	0.076	0.077	0.077
320 - 400	0.90	0.0020	0.0034	0.00094	0.0021	0.0024	0.089	0.089	0.089
400 - 900	0.90	0.0026	0.0024	0.0017	0.0028	0.0027	0.12	0.12	0.12

SHERPA 2.2.2

p_T^γ [GeV]	Purity	Stat Error	Syst Error					Total Syst Error	Total Error
			c_1	c_2	c_3	Isolation	Tightness		
150 - 170	0.86	0.00051	0.0062	0.00087	0.00099	0.0028	0.069	0.069	0.069
170 - 190	0.87	0.00068	0.0072	0.0012	0.0012	0.0027	0.066	0.066	0.066
190 - 210	0.88	0.00089	0.0046	0.00028	0.0011	0.0027	0.065	0.065	0.065
210 - 240	0.89	0.00097	0.0041	0.0018	0.0014	0.0025	0.066	0.066	0.066
240 - 280	0.89	0.0012	0.0030	0.0012	0.0015	0.0023	0.070	0.070	0.070
280 - 320	0.90	0.0018	0.0035	0.0014	0.0018	0.0025	0.076	0.077	0.077
320 - 400	0.90	0.0020	0.0034	0.00094	0.0021	0.0024	0.089	0.089	0.089
400 - 900	0.90	0.0026	0.0024	0.0017	0.0028	0.00275	0.12	0.12	0.12

Comparison Between Data and MC Simulations: PYTHIA

- Good Agreement between the Data after Background Subtraction and PYTHIA Simulation

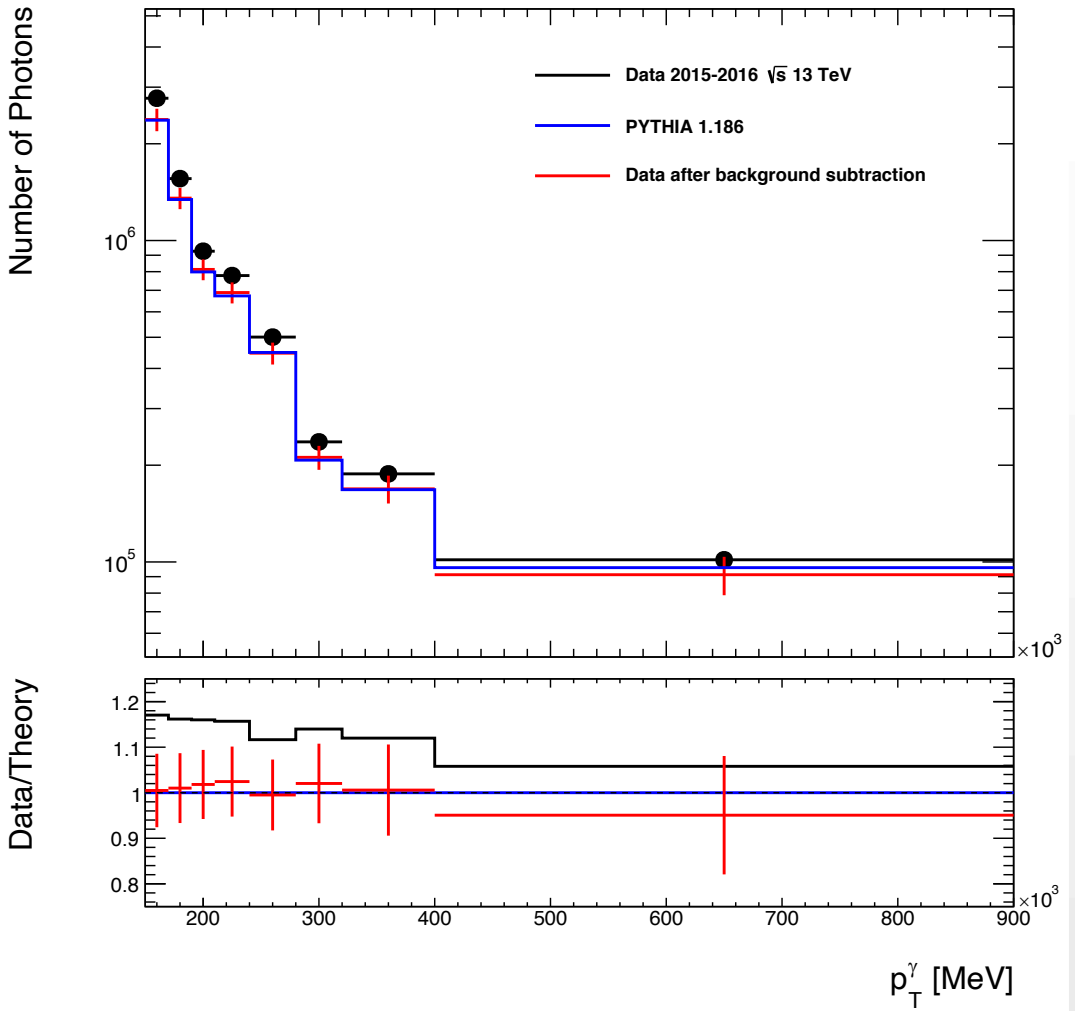

Comparison Between Data and MC Simulations: SHERPA

- Overestimation of the photon yield by SHERPA
- The distribution shape is consistent with the Data

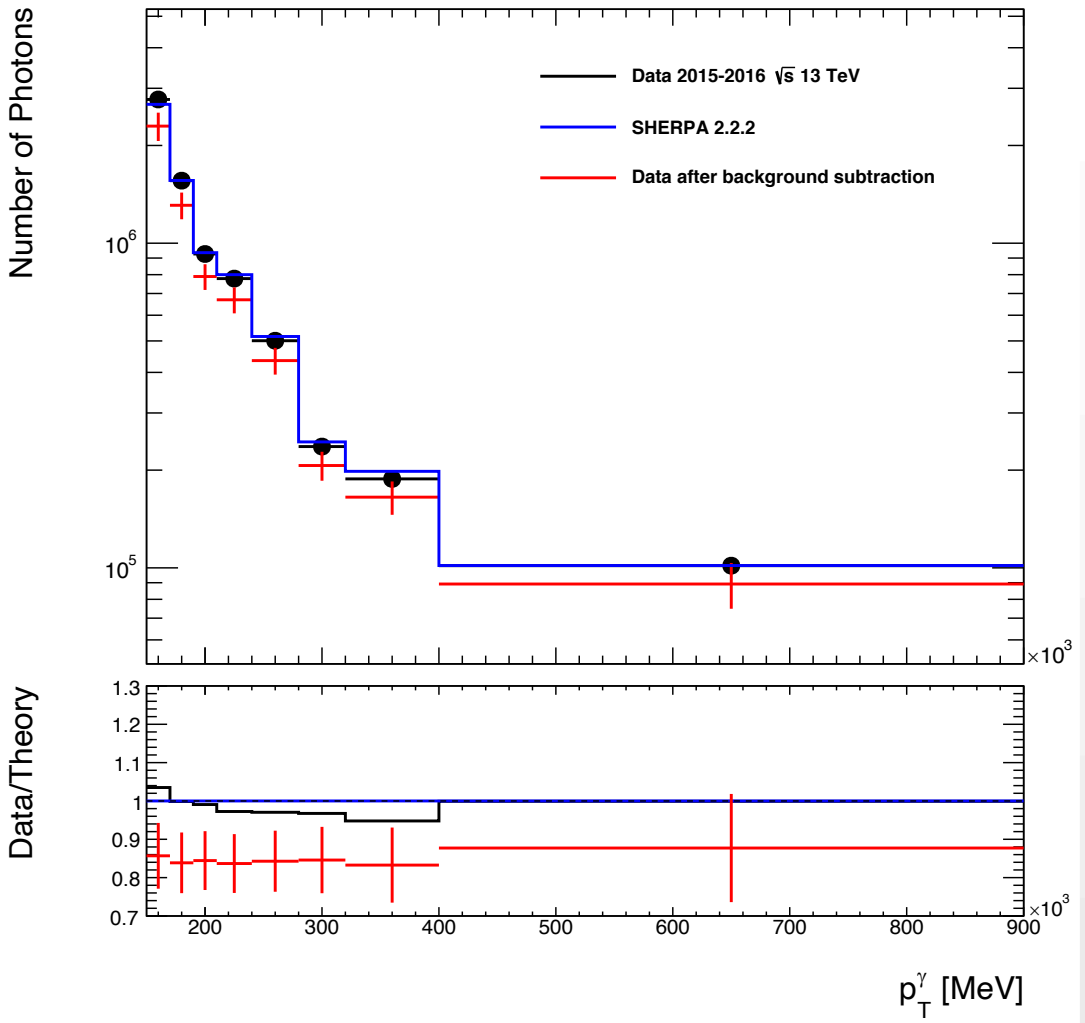

Conclusions

- The data collected in 2015 and 2016 by the ATLAS experiment with an integrated luminosity L_{int} = 36 fb^{-1} was confronted with the simulations performed by PYTHIA and SHERPA event generators.
- The background from jets faking photons was subtracted using the 2-Dimensional Sideband Method.
- The photon yields after background subtraction are well described by PYTHIA .
- On the contrary SHERPA seems to overestimate the event yields in data by ~ 15% on average although the shape of the p^{γ}_{T} distribution is well described.

Grazie per l’attenzione

Appendix: Cross Section and Luminosity

- Cross Section
  - It has the units of an area
  - It is related to the probability of an event to happen

- Luminosity
  - It is the proportionality factor between the cross section and the event rate
  - A high luminosity is necessary to observe an interaction with a small cross section

Appendix: Monte Carlo Event Generation

- Hard Process
- Parton Shower
- Hadronisation
- Underlying Event
- Decays of Unstable Particles
- Detector Simulation and Reconstruction

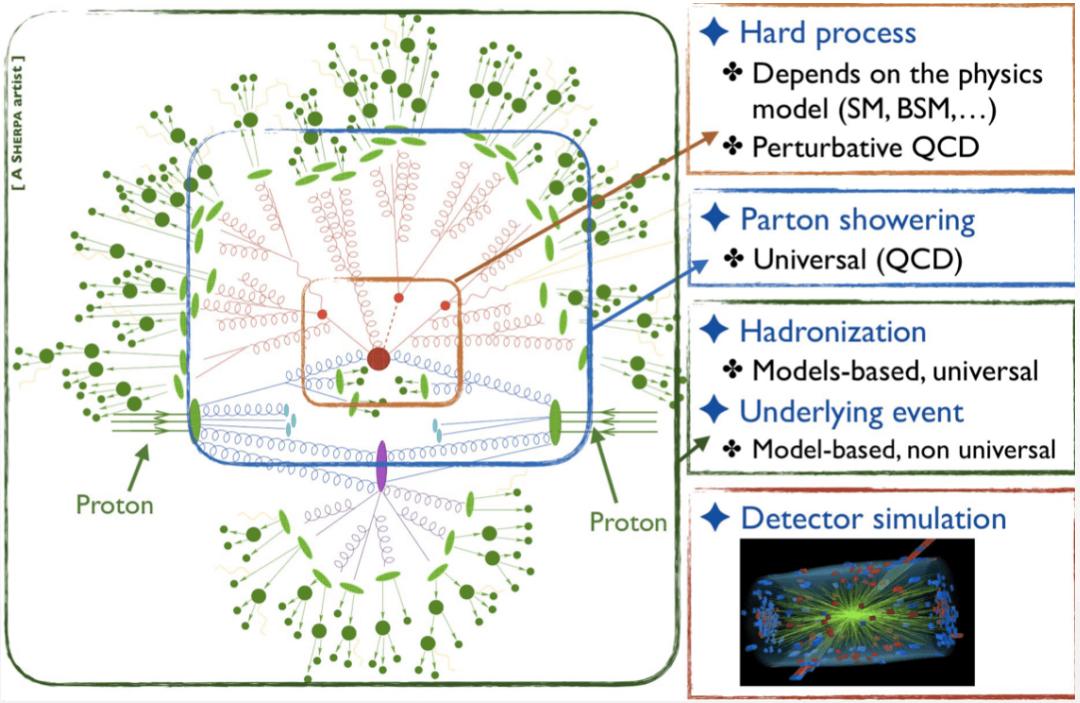

Appendix: The Electromagnetic Calorimeter

- Electromagnetic Calorimeter
  - Composed of two sections of the Liquid Argon Calorimeter, the Barrel ($|\eta| < 1.475$) and the End-Caps ($1.375 < |\eta| < 3.2$)
  - For $|\eta| < 2.5$ it is composed of three sampling layers, the first one being a high-granularity layer
- Made of two different materials
  - Active layers are made of liquid argon and interact with the particles, generating a shower
  - Passive layers are made of lead and collect the energy of the shower
- It has a nominal resolution for photons and electrons of $\frac{\sigma E}{E} \approx \frac{10\%-17\%}{\sqrt{E}} \oplus 0{,}7\%$

Appendix: Topo-Cluster Algorith

- Reconstruction happens through the dynamic Topo-Cluster algorithm

- Clusters are formed from proto-clusters, cells with significance $\varsigma_{cell}^{EM} = |\frac{E_{cell}^{EM}}{\sigma_{noise,cell}^{EM}}| \geq 4$. Neighboring cells with significance ≥ 2 are added to form a cluster.

- If a cluster satisfies $f_{EM}M = \frac{E_{L1}+E_{L2}+E_{L3}}{E_{CLUS}} > 0.5$, where E_{Li} is the energy deposited in a EM layer, it becomes a seed cluster.

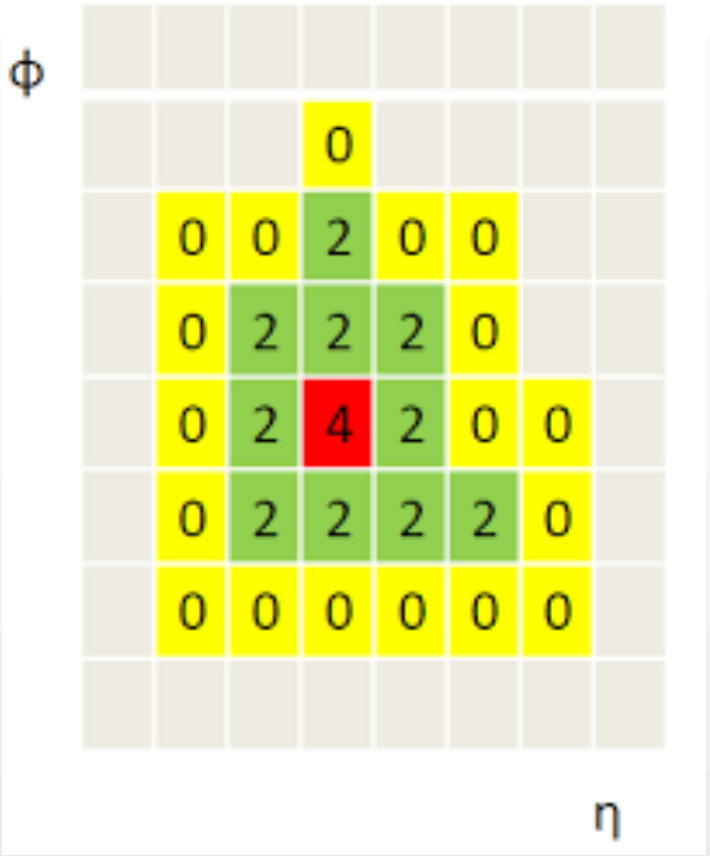

Appendix: Tight Selections

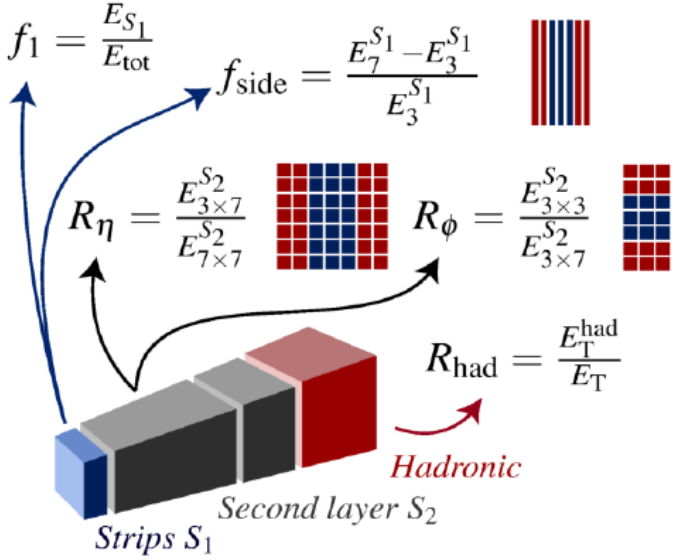

$$w_{\eta 2} = \sqrt{\frac{\Sigma E_i \eta_i^2}{\Sigma E_i} - \left(\frac{\Sigma E_i \eta_i}{\Sigma E_i}\right)^2}$$

width in a 3×5 ($\Delta\eta \times \Delta\phi$) region of cells in S_2

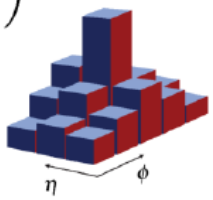

$$w_s = \sqrt{\frac{\Sigma E_i (i - i_{\max})^2}{\Sigma E_i}}$$

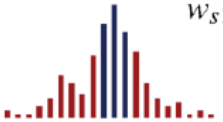

w_{s3} uses 3×2 strips ($\eta \times \phi$)

$w_{s\text{tot}}$ is defined similarly but uses 20×2 strips

$$\Delta E = E_{\text{max},2}^{S_1} - E_{\text{min}}^{S_1}$$

$$E_{\text{ratio}} = \frac{E_{\text{max},1}^{S_1} - E_{\text{max},2}^{S_1}}{E_{\text{max},1}^{S_1} + E_{\text{max},2}^{S_1}}$$

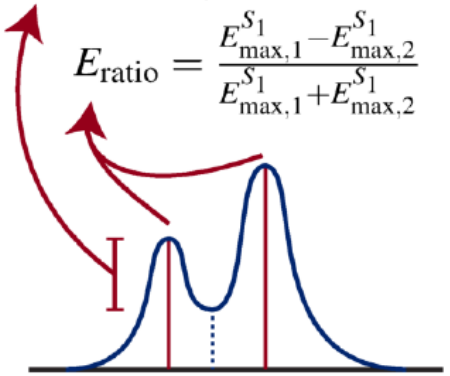

Appendix: PYTHIA Signal Leakage coefficients

Detector	p_T^γ [GeV]	c_1	$\sigma_{STAT}c_1$	c_2	$\sigma_{STAT}c_2$	c_3	$\sigma_{STAT}c_3$
Barrel	150 - 170	0.1106	0.0003	0.02842	0.00008	0.00860	0.00005
Barrel	170 - 190	0.1122	0.0004	0.0295	0.0001	0.01078	0.00008
Barrel	190 - 210	0.1042	0.0005	0.0301	0.0001	0.0114	0.0001
Barrel	210 - 240	0.1008	0.0005	0.0303	0.0001	0.01365	0.0001
Barrel	240 - 280	0.0948	0.0006	0.0321	0.0002	0.0158	0.0002
Barrel	280 - 320	0.0877	0.0008	0.0327	0.0003	0.0195	0.0002
Barrel	320 - 400	0.0809	0.0008	0.0339	0.0003	0.0221	0.0003
Barrel	400 - 900	0.0684	0.0009	0.0392	0.0005	0.0289	0.0004
End-Cap	150 - 170	0.1067	0.0004	0.0313	0.0002	0.01013	0.00009
End-Cap	170 - 190	0.1022	0.0005	0.0318	0.0002	0.0117	0.0001
End-Cap	190 - 210	0.0996	0.0006	0.0310	0.0003	0.0123	0.0002
End-Cap	210 - 240	0.0989	0.0007	0.0324	0.0003	0.0151	0.0002
End-Cap	240 - 280	0.0938	0.0008	0.0321	0.0004	0.0159	0.0003
End-Cap	280 - 320	0.085	0.001	0.0314	0.0006	0.0188	0.0004
End-Cap	320 - 400	0.079	0.001	0.0318	0.0007	0.0206	0.0005
End-Cap	400 - 900	0.068	0.002	0.033	0.001	0.0256	0.0009

Appendix: SHERPA Signal Leakage coefficients

Detector	p_T^γ [GeV]	c_1	$\sigma_{STAT}c_1$	c_2	$\sigma_{STAT}c_2$	c_3	$\sigma_{STAT}c_3$
Barrel	150 - 170	0.0980	0.0002	0.0289	0.0001	0.00430	0.00005
Barrel	170 - 190	0.0952	0.0003	0.0281	0.0002	0.00449	0.00006
Barrel	190 - 210	0.0931	0.0004	0.0295	0.0002	0.00451	0.00008
Barrel	210 - 240	0.0892	0.0004	0.0283	0.0002	0.00437	0.00009
Barrel	240 - 280	0.0849	0.0005	0.0299	0.0003	0.0044	0.0001
Barrel	280 - 320	0.0815	0.0007	0.0306	0.0004	0.0041	0.0001
Barrel	320 - 400	0.0756	0.0007	0.0320	0.0005	0.0043	0.0002
Barrel	400 - 900	0.0661	0.0009	0.0358	0.0006	0.0042	0.0002
End-Cap	150 - 170	0.1125	0.0004	0.0308	0.0002	0.00724	0.00009
End-Cap	170 - 190	0.1111	0.0005	0.0306	0.0002	0.0077	0.0001
End-Cap	190 - 210	0.1088	0.0006	0.0306	0.0003	0.0067	0.0001
End-Cap	210 - 240	0.1057	0.0006	0.0298	0.0003	0.0077	0.0002
End-Cap	240 - 280	0.1017	0.0008	0.0313	0.0004	0.0068	0.0002
End-Cap	280 - 320	0.096	0.001	0.0296	0.0006	0.0070	0.0003
End-Cap	320 - 400	0.089	0.001	0.0312	0.0007	0.0068	0.0003
End-Cap	400 - 900	0.074	0.002	0.029	0.001	0.0065	0.0005

Appendix: Correlation Factor for SHERPA

- Since the R coefficients shows fluctuasions in the different regions of the $\eta - p_T$ space due to the limited number of events in each region, it seemed more reasonable to use the value calculated over the whole data set

Detector	p_T^γ [GeV]	R_{MC}	$\sigma\ R_{MC}$	R_{MC}^{BARREL}	$\sigma\ R_{MC}^{BARREL}$	R_{MC}^{pT}	$\sigma\ R_{MC}^{pT}$	R_{MC}^{SB}	$\sigma\ R_{MC}^{SB}$	Events
Barrel	150 - 170	2.011	0.074	1.989	0.085	1.41	0.22	1.4	0.25	875.371
	170 - 190					2.00	0.31	1.54	0.31	955.182
	190 - 210					2.65	0.46	3.08	0.59	758.93
	210 - 240					1.78	0.28	2.0	0.35	958.943
	240 - 280					3.02	0.51	2.41	0.50	758.591
	280 - 320					1.03	0.23	0.93	0.24	541.697
	320 - 400					3.24	0.68	5.2	1.2	712.781
	400 - 900					2.31	0.58	1.75	0.48	538.146
Detector	p_T^γ [GeV]	R_{MC}	$\sigma\ R_{MC}$	R_{MC}^{ENDCAP}	$\sigma\ R_{MC}^{ENDCAP}$	R_{MC}^{pT}	$\sigma\ R_{MC}^{pT}$	R_{MC}^{SB}	$\sigma\ R_{MC}^{SB}$	**Events**
End-Cap	150 - 170	2.011	0.074	2.04	0.15	1.41	0.22	1.52	0.50	258.699
	170 - 190					2.00	0.31	3.024	0.85	347.645
	190 - 210					2.65	0.46	1.42	0.59	225.495
	210 - 240					1.78	0.28	1.18	0.43	248.469
	240 - 280					3.02	0.51	4.4	1.4	229.553
	280 - 320					1.03	0.23	1.39	0.64	144.516
	320 - 400					3.24	0.63	0.72	0.30	145.518
	400 - 900					2.31	0.58	10.5	7.1	94.8555

Appendix: R prime

- Validity of the MC simulations for 2-Dimensional Sideband Method
  - Necessary to check if the MC simulation is a good approximation of the data
  - The factor R is evaluated over a highly non-isolated region for the data and the MC simulations and the two are compared
  - It is denominated R'

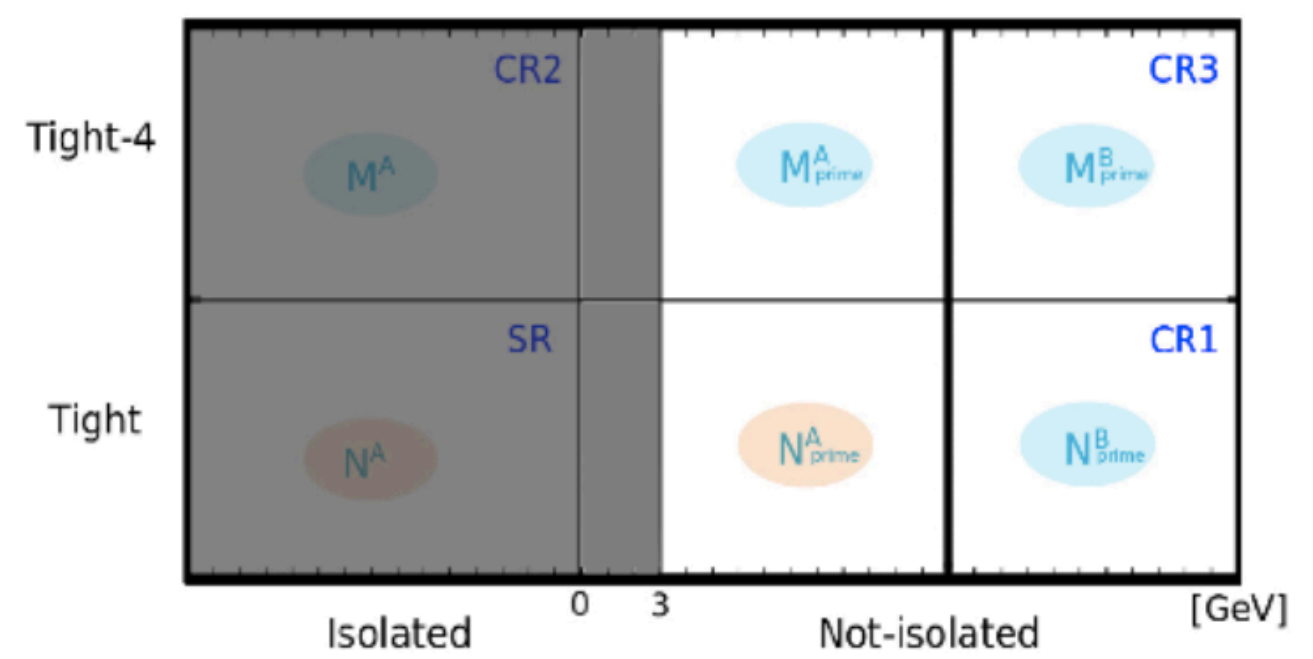

Appendix: R prime PYTHIA

Detector	p_T^γ [GeV]	R'_{DATA}	$\sigma R'_{DATA}$	R'^{SB}_{DATA}	$\sigma R'^{SB}_{DATA}$	R'_{PYTHIA}	$\sigma R'_{PYTHIA}$	R'^{SB}_{PYTHIA}	$\sigma R'^{SB}_{PYTHIA}$	Events
Barrel	150 - 170	1.0167	0.0017	0.9669	0.0033	1.05	0.06	0.97	0.17	1004.88
	170 - 190			0.9955	0.0043			1.55	0.28	1101.58
	190 - 210			1.02	0.0054			1.24	0.23	928.494
	210 - 240			1.0491	0.0058			0.93	0.15	1091.63
	240 - 280			1.0707	0.0070			0.77	0.12	1138.72
	280 - 320			1.0740	0.0098			0.90	0.16	867.477
	320 - 400			1.152	0.011			0.94	0.17	929.398
	400 - 900			1.145	0.015			0.70	0.13	941.057
End-Cap	150 - 170	1.0167	0.0017	0.9110	0.0048	1.05	0.06	1.18	0.34	358.521
	170 - 190			0.9293	0.0061			1.74	0.52	338.838
	190 - 210			0.9456	0.0077			1.21	0.36	357.465
	210 - 240			0.9514	0.0082			0.77	0.26	347.606
	240 - 280			0.99	0.010			1.55	0.42	342.481
	280 - 320			1.018	0.015			0.63	0.22	233.061
	320 - 400			1.044	0.018			5.8	2.2	246.089
	400 - 900			1.040	0.028			1.41	0.59	180.53

Appendix: R prime SHERPA

Detector	p_T^γ [GeV]	R'_{DATA}	$\sigma R'_{DATA}$	R'^{SB}_{DATA}	$\sigma R'^{SB}_{DATA}$	R'_{SHERPA}	$\sigma R'_{SHERPA}$	R'^{SB}_{SHERPA}	$\sigma R'^{SB}_{SHERPA}$	Events
Barrel	150 - 170	1.0167	0.0017	0.9669	0.0033	0.822	0.053	0.95	0.20	875.371
	170 - 190			0.9955	0.0042			0.54	0.10	955.182
	190 - 210			1.0221	0.0054			0.68	0.15	758.93
	210 - 240			1.0491	0.0058			0.90	0.17	958.943
	240 - 280			1.0707	0.0070			1.39	0.31	758.591
	280 - 320			1.074	0.0098			0.56	0.13	541.697
	320 - 400			1.152	0.011			0.78	0.18	712.781
	400 - 900			1.145	0.015			0.88	0.20	538.146
End-Cap	150 - 170	1.0167	0.0017	0.9110	0.0048	0.822	0.053	1.23	0.44	258.699
	170 - 190			0.9293	0.0060			0.91	0.27	347.645
	190 - 210			0.9456	0.0077			0.27	0.12	225.495
	210 - 240			0.9515	0.0082			0.99	0.33	248.469
	240 - 280			0.99	0.01			1.40	0.57	229.553
	280 - 320			1.018	0.015			1.15	0.54	144.516
	320 - 400			1.044	0.018			1.80	0.75	145.518
	400 - 900			1.040	0.028			2.0	1.2	94.8555